



Dysregulated *KRAS* gene-signaling axis and abnormal chromatin remodeling drive therapeutic resistance in heterogeneous-sized circulating tumor cells in gastric cancer patients

Yang Chen^{a,1}, Yanyan Li^{a,1}, Changsong Qi^a, Cheng Zhang^a, Dan Liu^a, Youping Deng^b, Yuanyuan Fu^b, Vedbar S. Khadka^b, Daisy Dandan Wang^c, Shanyang Tan^d, Shujun Liu^d, Zhi Peng^a, Jifang Gong^a, Peter Ping Lin^c, Xiaotian Zhang^a, Jian Li^a, Yilin Li^{a,*}, Lin Shen^{a,**}

^a Department of Gastrointestinal Oncology, Key Laboratory of Carcinogenesis and Translational Research (Ministry of Education), Peking University Cancer Hospital and Institute, Beijing, China

^b Bioinformatics Core, Department of Quantitative Health Sciences, John A. Burns School of Medicine, University of Hawaii, Honolulu, HI, USA

^c Cytelligen, San Diego, CA, USA

^d Jiangsu Cowin Biotech Co., Ltd, China Medical City, Taizhou, Jiangsu, China

ARTICLE INFO

Keywords:

Circulating tumor cells
Gastric cancer
Size heterogeneity
Single-cell DNA sequencing
Therapeutic resistance

ABSTRACT

The mechanism by which heterogeneous-sized circulating tumor cells (CTCs) in gastric cancer (GC) patients are resistant to the targeted therapy and/or chemotherapy remains unclear. This study investigated prognostic value and genomic variations of size-heterogeneous CTCs, in an attempt to unravel the molecular mechanisms underlying the therapeutic resistance, which is relevant to poor prognosis in GC. Aneuploid CTCs, detected in 111 advanced GC patients, were categorized into small (\leq white blood cell [WBC], 25.54%) and large ($>$ WBC, 74.46%) cells. Pre-treatment patients possessing ≥ 3 baseline small CTCs with trisomy 8 ($sCTCs^{tri}$) or ≥ 6 large multiploid CTCs ($lCTCs^{multi}$) showed an inferior median progression-free survival. Moreover, the cut-off value of ≥ 6 $lCTCs^{multi}$ was also an effective prognosticator for poor median overall survival. Single cell-based DNA sequencing of 50 targeted CTCs indicated that $sCTCs^{tri}$ and $lCTCs^{multi}$ harbored distinct gene variations respectively. Mutations in the *KRAS* and *Rap1* pathway were remarkably abundant in $sCTCs^{tri}$, whereas several unique mutations in the *MET/PI3K/AKT* pathway and *SMARCB1* gene were identified in $lCTCs^{multi}$. Obtained results suggested that $sCTCs^{tri}$ and $lCTCs^{multi}$ exhibited different mechanisms to therapy resistance and correlated with patients' poor outcome.

1. Introduction

Circulating tumor cells (CTCs) are highly variable in phenotype, genotype, and cell size. The excessive heterogeneity of CTCs fosters the escape of tumor cells from immune surveillance and therapeutic pressures, resulting in facilitated distant metastasis and tumor relapse [1,2]. Great efforts have been made to unravel the molecular characteristics of CTCs to target therapeutic resistance, the metastatic process and the recurrence of cancers [3,4].

Aneuploidy, one of the hallmarks of malignant neoplastic cells [5,6], has been recognized to relate to genomic instability and the development of tumoral drug resistance [7]. The examination of aneuploid chromosome 8 (chr8) by the centromere probe 8 (CEP 8) to identify solid tumor cells has been approved by the USFDA (United States Food and Drug Administration). In particular, diverse copy numbers of aneuploid chr8 in CTCs were found to correlate with the intrinsic and acquired chemo-resistance in gastric cancer (GC) patients [8]. Moreover, multiploid chr8 also participated in the acquisition of human epidermal

* Corresponding author. Department of Gastrointestinal Oncology, Key Laboratory of Carcinogenesis and Translational Research (Ministry of Education), Peking University Cancer Hospital and Institute, Fucheng Road 52, Haidian District, Beijing, 100142, China.

** Corresponding author. Department of Gastrointestinal Oncology, Key Laboratory of Carcinogenesis and Translational Research (Ministry of Education), Peking University Cancer Hospital and Institute, Fucheng Road 52, Haidian District, Beijing, 100142, China.

E-mail addresses: liyilin@bjcancer.org (Y. Li), shenlin@bjmu.edu.cn (L. Shen).

¹ These authors contributed equally.

growth factor receptor 2 (HER2) phenotype on GC CTCs. This provides a growth advantage for neoplastic cells against therapeutic pressure, leading to the development of resistance to either chemotherapy alone [8] or chemotherapy plus targeted therapy [9] in GC patients. In addition to chromosome aneuploidy, mutations in several oncogenes in cancer cells have demonstrated their association with therapeutic resistance in a variety of carcinoma patients. For instance, a higher degree of aneuploidy is associated with a higher frequency of *KRAS* (Kirsten rat sarcoma 2) and *TP53* (Tumor Protein 53) mutations in colorectal cancer [5]. *KRAS* activation promotes epithelial-to-mesenchymal transition (EMT), which facilitates the transition of malignant cells to cancer stem-like cells (CSCs) and hence promotes metastasis [10]. Phosphatidylinositol-4, 5-bisphosphate 3-kinase catalytic subunit alpha (*PIK3CA*) mutations negatively impact the effectiveness of trastuzumab-based chemotherapy in GC [11].

Aside from molecular heterogeneity, CTCs also notably display heterogeneous morphology in both large and small cell sizes [12], and each category of cells possesses distinct clinical utility. In contrast to large CTCs (\geq WBCs, $>$ white blood cell (WBC)), the small cell size CTCs (\leq WBC) are known to be relevant to anti-apoptosis [13], EMT [14], resistance to immunotherapy [15], cancer metastasis and progression [16] as well as post-surgical recurrence [17]. This suggests that underlying molecular mechanisms, which are yet to be elucidated, impact and regulate CTCs' size plasticity, thus exhibiting clinical significance including either intrinsic or acquired resistance to therapeutic regimens.

In the present study, extending beyond our previous studies [8,9,18,19], we took advantage of cell nuclear size and the surface molecule-independent subtraction enrichment (SE)-iFISH strategy to comprehensively co-investigate how cell morphology and karyotype, in terms of small and large cell size CTCs bearing different copy numbers of chr8, correlate with GC patients' prognosis, including progression-free survival (PFS) and overall survival (OS). Furthermore, single-cell sequencing (SCS) was performed on the targeted GC \leq CTCs and \geq CTCs to pinpoint the unique genetic variants, in an effort to explore the mechanisms regarding how therapeutic resistance is developed in different sizes of CTCs in GC patients.

2. Materials and methods

2.1. Patient enrollment and specimen collection

A total of 111 advanced GC patients were enrolled at the Peking University Cancer Hospital from January 2015 to February 2017. All patients (\geq 18 years-old), with Karnofsky performance status (KPS) \geq 70, had locally advanced, recurrent, and/or histopathologically confirmed metastatic adenocarcinoma at either stomach or gastroesophageal junction. Patients were subjected to first-line paclitaxel or cisplatin-based chemotherapy with or without trastuzumab based upon histopathological HER2 status. Our cohort was first described in a previous study [9], in which we excluded four patients with double primary tumors.

Clinical responses were evaluated once in every six weeks by computed tomography (CT) scanning according to the Response Evaluation Criteria in Solid Tumors (RECIST, version 1.1). Responses were categorized as stable disease (SD), partial response (PR) or progressive disease (PD). Censoring occurred if patients were still alive at last follow-up.

Six milliliters (ml) of blood was periodically collected from all the recruited 111 patients at baseline. Among 111 subjects, 103 of them received longitudinal CTC assessment performed right before the beginning of each treatment cycle. The remaining eight patients were not available for the scheduled post-therapeutic assessments due to unforeseen clinical complications.

Consent forms signed by all subjects were approved by the Ethics Review Committees of Peking University Cancer Hospital, Beijing, China. The written consent forms were received from each patient prior

to blood collection. The clinical study was performed according to the principles of the Declaration of Helsinki.

2.2. SE-iFISH and single cell collection

The experiment was performed according to the manufacturer's protocol (Cytelligen, San Diego, CA, USA) with minor modifications [9]. Briefly, six ml of peripheral blood was collected into a tube containing ACD anti-coagulant (Becton Dickinson, Franklin Lakes, NJ, USA). Blood samples were centrifuged at $200\times g$ for 15 min at room temperature. Sedimented blood cells were gently mixed with 3.5 ml of hCTC buffer, loaded on the non-hematopoietic cell separation matrix in a 50 ml tube, and subsequently centrifuged at $450\times g$ for 5 min. The entire solution containing WBCs and tumor cells above the red blood cell (RBC) layer was collected into a 50 ml tube, and subsequently incubated with 300 μ l of immuno-magnetic beads conjugated to a cocktail of anti-leukocyte mAbs at room temperature for 30 min. WBCs bound to immuno-beads were depleted using a magnetic separator. Solutions free of magnetic beads were collected and spun at $500\times g$ for 4 min. Sedimented cells were subjected to subsequent iFISH.

Dried monolayer cells on the coated CTC slides were hybridized with CEP8 Spectrum Orange (Vysis, Abbott Laboratories, Chicago, IL, USA). Samples were subsequently incubated with anti-CD45 monoclonal antibody conjugated to Alexa Fluor (AF) 594. After washing, samples were mounted with mounting media and subjected to the automated Metafer-iFISH® CTC 3D scanning and image analysis system co-developed by Carl Zeiss (Oberkochen, Germany), MetaSystems (Altlusheim, Germany) and Cytelligen [18]. Fluorescence in situ hybridization (FISH) was performed using centromere probe 8 (CEP8, Vysis and Abbott, Abbott Park, IL, USA). CTCs with $>$ disomy 8 were defined as aneuploid. CTCs were defined as DAPI⁺ and CD45⁻ with aneuploid Chr8.

Isolation of the targeted aneuploid \leq CTCs and \geq CTCs identified by iFISH was performed by means of a non-laser microscopic single cell manipulator (NMSCM, Cytelligen) as previously described [9].

2.3. Whole-genome amplification and next generation sequencing of the single CTCs

The whole-genome amplification of single CTCs was performed using Single Cell WGA Kit (MDA) (CWbio, Beijing, China) according to the manufacturer's instructions. Following the MDA reaction, clean up was performed using MagBead DNA Purification Kit (CWbio, Beijing, China). Briefly, 100 μ L of CMPure beads was added to each sample (50 μ L) according to the manufacturer's instructions, and in the last step, beads were resuspended in 70–100 μ L of nuclease-free water (pH 8). The cleaned-up products were subsequently moved to a new PCR plate. These MDA products were quantified using the Quant-IT PicoGreen dsDNA assay kit (Invitrogen), and products with concentrations greater than the negative control were selected for next generation sequencing. After whole-genome amplification of the genome of a single CTC and MDA products clean up, qPCR was performed for 8 randomly selected loci (Supplementary Table S1) to check the genomic integrity of the whole-genome amplification product. DNA samples with five of eight loci amplified by qPCR with a reasonable Ct number (Ct = 20–35) were used for subsequent analyses. Among the CTCs that failed to meet the criteria for inclusion, most did not show a reasonable Ct number at all eight loci, which indicated failure to transfer CTCs to the PCR tube during the micro-pipetting step.

For each CTC sample, cancer hotspot panel (50 targeted genes) libraries were prepared using the TarSight Tumor 50 Library Prep Kit (CWbio), quantified using the Library Quantification Kit for Illumina (Kapa Biosystems), and sequenced by an Illumina HiSeq X Ten system (read lengths of 2 x 150 bp).

2.4. Detection of short variant

Adapters and low-quality bases (Phred score below 20) were trimmed off using Trim Galore. Reads were aligned to the human reference genome hg19 using BWA-MEM and default parameters. Local realignment and base quality recalibration (BQR) were performed using the GATK. Alignment and coverage metrics as well as PCR duplicate marking were computed using Picard tools.

Somatic short variants were called by Mutect2 with default parameters. We included all mutations that passed all the internal filters as well as mutations that failed the “clustered_events” and “homologous_mapping_event” filters. Annotation of mutations and effect prediction were done using SnpEff. It annotates and predicts the effects of variants on genes (such as amino acid changes). Clinical mutations were also associated with Catalogue of Somatic Mutations in Cancer (COSMIC) Ids.

2.5. Statistical analysis

For survival analysis, all statistical analyses were performed with SPSS 21.0 software (IBM Corp., New York, USA). PFS was defined as the time from initial treatment to the date that clinical progression was confirmed or was censored at the last follow-up. OS was defined as the time from initial treatment to the date that death occurred or was censored at the last follow-up. Kaplan–Meier survival plots for PFS or OS were generated based on the number of CTCs, and the survival curves were compared using log-rank tests. Cox proportional hazards regression was used to determine the hazard ratios of PFS or OS under different cutoff values of CTCs. Comparison of significant mutations between heterogeneous-sized CTCs was done using non-parametric tests such as Fisher’s exact test, based on the binary mutation profiles. G: Profiler was used for significantly mutated pathways (SMPs) analysis [20,21]. Exclusively mutated genes in heterogeneous-sized CTCs were respectively treated as an unordered query, and statistical tests were conducted based on the KEGG data sources. All the *P* values are two-sided. **P*-values < 0.05 were considered statistically significant.

3. Results

3.1. Small size CTCs with trisomy 8 ($sCTCs^{tri}$) and large size multiploid CTCs ($lCTCs^{multi}$) are dominant CTC components in GC

Chr8 karyotypic characteristics in both non-hematologic $sCTC$ (≤ 5 μm nuclear size of WBC) and $lCTCs$ (> 5 μm nuclear size of WBC) were profiled in all 111 patients. Aneuploid chr8 in CTCs, i.e., triploid 8 (3 copies of chr8), tetraploid 8 (4 copies of chr8) and multiploid 8 (≥ 5 copies of chr8) were examined (Fig. 1A). Among those subjects, 62 of them received chemotherapy alone, and 49 patients received trastuzumab plus chemotherapy. The clinical characteristics of enrolled GC patients is shown in Table 1. Out of 111 patients, 102 subjects had ≥ 1 CTC detected (102/111 = 91.9%), with a median value of 10 cells (Interquartile range (IQR): 3–28.5/6 ml) (Table 1). Among those 102 patients, 79 subjects had both $sCTCs$ and $lCTCs$, 10 patients had only $sCTCs$, and the remaining 13 patients had $lCTCs$ detected exclusively. As shown in Fig. 1B, out of 13226 CTCs, 25.54% (3378 out of 13226) were $sCTCs$ and the remaining 74.46% (9848 out of 13226) were in large cell size.

The clinical relevance of $sCTCs$ was investigated. As shown in Fig. 1C and Supplementary Table S2, 80% of patients exclusively possessing $sCTCs$ experienced liver metastasis compared to 38.5% in patients exclusively having $lCTCs$ (Fig. 1C). This shows that the presence of $sCTCs$ correlates with hepatic metastasis. Further insight into the karyotype composition indicated that trisomy 8 constituted the highest percentage (65.93%) of $sCTCs$ ($sCTCs^{tri}$), whereas the largest proportion (73.09%) of $lCTCs$ were multiploid (≥ 5 copy numbers of Chr 8, $lCTCs^{multi}$) (Fig. 1D).

3.2. $sCTCs^{tri}$ and $lCTCs^{multi}$ predominately contribute to therapeutic resistance and poor prognosis in GC patients

Next, the clinical significance of the quantitative $sCTCs^{tri}$ and $lCTCs^{multi}$ at baseline was further evaluated. The correlation of pre-therapeutic total CTCs, $sCTCs$ and $lCTCs$ bearing different chr8 ploidies with GC patients’ PFS and OS is shown in Fig. 2 and Supplementary Figs. S1A and B. Both increased $sCTCs^{tri}$ with a cut-off value of 1 or 3 cells (Fig. 2A), and $lCTCs^{multi}$ with a cut-off of 4, 5 or 6 cells (Fig. 2B) exhibited the most significant correlation with the shorter PFS. Although quantities ≥ 2 $sCTCs^{multi}$ or ≥ 1 $lCTCs^{tetra}$ also showed significant correlation with inferior PFS, the percentages of these two subtypes of CTCs at baseline and PD were too low (Figs. 1C and 2A and B). Therefore, $sCTCs^{tri}$ and $lCTCs^{multi}$ are the significant major subtypes involved in poor PFS and development of chemo/targeted therapy resistance in GC patients.

Kaplan–Meier curves of PFS in cohorts containing $sCTCs^{tri}$ and $lCTCs^{multi}$ are illustrated in Fig. 2C and D. As shown in Fig. 2C, the median PFS (mPFS) of patients with ≥ 3 $sCTCs^{tri}$ was 3.13 months (95% CI: 2.54–3.73 months) compared to 4.70 months (95% CI: 3.92–5.48 months) in patients containing < 3 $sCTCs^{tri}$ (**P* = 0.019). As shown in Fig. 2D, patients possessing ≥ 6 $lCTCs^{multi}$ had a mPFS of 3.13 months (95% CI: 1.56–4.70 months) which was significantly shorter than 4.70 months (95% CI: 3.87–5.53 months) in patients having < 6 $lCTCs^{multi}$ (**P* = 0.037). Additional analysis in Fig. 2E demonstrated that ≥ 6 $lCTCs^{multi}$ (median OS (mOS): 10.3 months [95% CI: 9.50–11.10 months] vs. 17.80 months [95% CI: 13.71–21.90 months]) rather than $sCTC^{tri}$ is a prognosticator for lower OS (Supplementary Fig. S1C).

Further analysis of longitudinal variation of $sCTCs^{tri}$ and $lCTCs^{multi}$ following chemo/targeted therapy resistance developed in 53 patients (53/111 = 47.75%) is depicted in Fig. 3A and B. Increase in both total quantity and average number of $sCTCs^{tri}$ (A) and $lCTCs^{multi}$ (B) in PD patients was observed. Obtained results were further supported by the individuals’ progression heatmap analysis (Fig. 3C and D), showing that both $sCTCs^{tri}$ and $lCTCs^{multi}$ were the major subtypes elevated in PD patients.

Taken together, obtained results imply that both the $sCTCs^{tri}$ and $lCTCs^{multi}$ significantly correlated with chemo/targeted therapy resistance in GC patients.

3.3. $sCTCs^{tri}$ harbor mutated KRAS gene and $lCTCs^{multi}$ possess MET and SMARCB1 mutational signatures identified by the single cell sequencing

The karyotypic characteristics of $sCTCs$ and $lCTCs$ and their distinct roles in chemo-/targeted therapeutic resistance and prognosis lead us to hypothesize that undefined molecular mechanisms may underlie the regulation of the size heterogeneity of CTCs in GC. To illustrate the molecular heterogeneity between $sCTCs$ and $lCTCs$, 50-gene (Supplementary Table S3) targeted SCS was respectively performed on each of the 53 single CTCs including 28 $sCTCs^{tri}$ and 25 $lCTCs^{multi}$ from six treatment-naïve HER2-negative patients. Among six patients, two subjects had the available paired primary tumor, $sCTCs^{tri}$ and $lCTCs^{multi}$. Mutations in the primary tumor were examined by the targeted bulk sequencing.

To demonstrate that diverse subtypes of CTCs detected by SE-iFISH originated from the same primary tumor, seven $sCTCs^{tri}$ and four $lCTCs^{multi}$ from the two patients with their matched primary tumor specimens were subjected to next-generation sequencing. As shown in Fig. 4A, $sCTCs^{tri}$, $lCTCs^{multi}$ and the primary tumor revealed 23, 31 and 12 gene variations, respectively. Seven out of twelve gene variations (58.33%) in the primary tumor were shared by $sCTCs^{tri}$ or $lCTCs^{multi}$, suggesting that $sCTCs^{tri}$ and $lCTCs^{multi}$ originated from the same primary tumor. The neoplastic cells, shed from primary lesion into peripheral circulation, may undergo further evolution to acquire heterogeneous genetic alternations and cell morphologies.

To investigate whether particular genetic alternations may associate

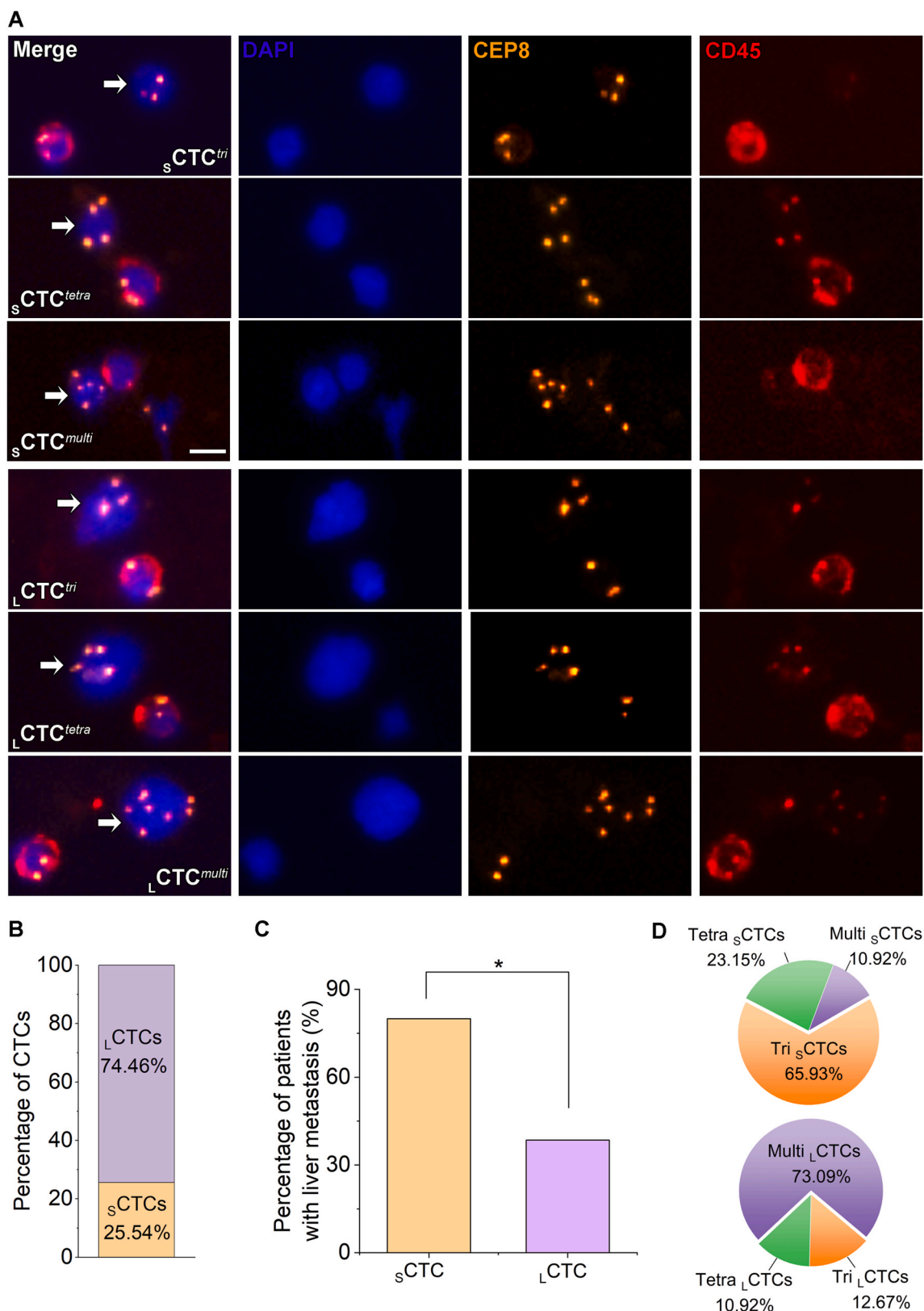


Fig. 1. Circulating gastric cancer cells in heterogeneous sizes. (A) Typical images of aneuploid small CTCs (sCTCs, \leq WBC, white arrows in upper three panels) and large CTCs (LCTCs, $>$ WBC, white arrows in lower three panels). CD45⁺ cells in each image are WBCs. The anti-CD45 antibody is used to exclude WBCs in this experiment. Bar, 5 μ m. (B) The histogram represents percentages of sCTC or LCTC in all the detected CTCs. (C) The percentages of patients with hepatic metastasis in exclusively sCTC-positive (N = 10) or LCTC-positive patients (N = 13). *P = 0.046 (D) Pie charts represent the proportions of triploid, tetraploid and multiploid chr8 in sCTCs (C) or LCTCs (D) in all the detected sCTCs or LCTCs.

Table 1
Clinical characteristics of enrolled advanced GC patients.

Characteristics*	ALL (N = 111)
Gender	
Male	92 (82.9%)
Female	19 (17.1%)
Age (Years)	
<60	44 (39.6%)
≥60	67 (60.4%)
Location	
Non-GEJ	65 (58.6%)
GEJ	46 (41.4%)
Lauren classification	
Intestinal	66 (59.5%)
Diffuse	15 (13.5%)
Mixed	21 (18.9%)
Unknown	8 (7.2%)
Liver metastasis	
Yes	59 (53.1%)
No	52 (46.9%)
Lung metastasis	
Yes	17 (15.3%)
No	94 (84.7%)
Peritoneal metastasis	
Yes	15 (13.5%)
No	96 (86.5%)
Bone metastasis	
Yes	12 (10.8%)
No	99 (89.2%)
Treatment regimen	
Trastuzumab combined chemotherapy	49 (44.1%)
Chemotherapy alone	62 (55.9%)
CTC (Median, IQR)	10 (3–28.5)
sCTC (Median, IQR) (N = 87)	3 (1–6.5)
sCTC ^{tri} (Median, IQR) (N = 79)	2 (0–5)
sCTC ^{tetra} (Median, IQR) (N = 56)	0 (0–1)
sCTC ^{multi} (Median, IQR) (N = 30)	0 (0–1)
lCTC (Median, IQR) (N = 86)	6 (2–20.5)
lCTC ^{tri} (Median, IQR) (N = 55)	0 (0–2)
lCTC ^{tetra} (Median, IQR) (N = 51)	0 (0–2)
lCTC ^{multi} (Median, IQR) (N = 85)	5 (1–16.5)

*Abbreviations: GEJ: esophagogastric junction; CTC: circulating tumor cell; sCTC: small size CTC; lCTC: large size CTC; sCTC^{tri}: triploid sCTC; sCTC^{tetra}: tetraploid sCTC; sCTC^{multi}: multiploid sCTC; lCTC^{tri}: triploid lCTC; lCTC^{tetra}: Tetraploid lCTC; lCTC^{multi}: multiploid lCTC; IQR: inter-quartile range.

with cell size variation and karyotypic plasticity of CTCs, systemic comparison was performed on the identified mutations obtained from 28 sCTCs^{tri} and 25 lCTCs^{multi}, including all the point mutations, insertion and deletions (Indels) (Supplementary Table S4). As shown in Fig. 4B, several mutations including 14 non-synonymous mutations, two synonymous mutations, and two stop-gain mutations were respectively identified in sCTCs^{tri} and lCTCs^{multi}. The difference, in terms of the identified specific gene or the numbers of mutations on the same gene, between the two categories of cells was statistically significant (*P < 0.05). Percentages of cells with the significantly different genetic variants in sCTCs^{tri} or lCTCs^{multi} were compared in Fig. 4C. In particular, KRAS A18V, G15S and V7A non-synonymous mutations were more frequently identified in sCTCs^{tri}, and high frequency of MET E1214A, E1214D, K1215E, K1215 N, F1216L, FGFR1 M2761, PIK3CA K440 N, and L687I mutations, however, were detected in lCTCs^{multi}. As summarized in Fig. 4D, higher KRAS mutations were identified in sCTCs^{tri}, whereas lCTCs^{multi} had higher MET mutations. SMARCB1 mutations, identified exclusively in lCTCs^{multi} only, may play a significant role in regulating the clinical and biological functions of lCTCs^{multi}.

3.4. Dysregulation of KRAS related-GTPase pathway in sCTCs^{tri} and abnormal SMARCB1-mediated chromatin remodeling in lCTCs^{multi} drive development of therapeutic resistance in GC patients

To further compare significantly mutated pathways (SMP) related to therapeutic resistance in sCTCs^{tri} and lCTCs^{multi}, the distribution of

differentiated mutated genes was examined across Kyoto Encyclopedia of Genes and Genomes (KEGG) pathways (Fig. 4E and F, Supplementary Tables S5 and S6). Top 10 SMPs in sCTCs^{tri} and lCTCs^{multi} were respectively illustrated in Fig. 4E and F. Aside from common pathways in cancer and cancer carbon metabolisms, sCTCs^{tri} and lCTCs^{multi} also exhibited different SMPs. In sCTCs^{tri}, mutated genes with high frequency were identified in the Rap1 signaling pathway, whereas, in lCTCs^{multi}, an abundance of gene mutations was found in PI3K/AKT signaling pathway. RAP1 is a small GTPase which has high sequence similarity to another small GTPase, RAS, and both are involved in treatment-resistance in cancers [22]. In sCTCs^{tri}, existence of enriched mutant genes in the RAP1 pathway (Fig. 4E) and a high frequency of KRAS mutations indicate that small GTPase-mediated pathways primarily contribute to chemo-/targeted therapy resistance (Fig. 5). Regarding lCTCs^{multi}, in addition to the active treatment-resistance PI3K/AKT pathway, mutant SMARCB1 was exclusively identified in this category of cells. This mutation plays an important role in chromatin remodeling and transcriptional regulation [23], which implies that abnormal chromatin remodeling might also contribute to therapeutic resistance in lCTCs^{multi} (Fig. 5). Obtained results indicated that sCTCs^{tri} and lCTCs^{multi} respectively harbor distinct therapeutic resistance mechanisms involving diverse signaling pathways.

4. Discussion

It has been reported that CTCs in heterogeneous sizes correlated with distant metastatic sites and prognosis in prostate cancer [16] and hepatocellular cancer [17]. However, molecular mechanisms underlying how CTCs' size heterogeneity correlates to CTCs' dissemination and resistance to therapy remains unclear. Accordingly, genomic mechanisms in terms of heterogeneous-sized GC CTCs' chemotherapeutic resistance were systematically investigated in the present study.

Extending beyond our previous discoveries showing that the karyotypic plasticity in Chr8 is involved in the acquisition of HER2 phenotype in GC [9], we further demonstrated in the current study that GC sCTCs and lCTCs bear distinct karyotypic features. Trisomy 8 and multिसomy 8 respectively constitute the principal karyotype in sCTCs (sCTCs^{tri}) and lCTCs (lCTCs^{multi}). Both particular subtypes of CTCs predominantly contribute to chemo-/targeted therapeutic resistance in GC patients.

Taking advantage of single CTC-based DNA sequencing, we explored genetic variation profiling in individual sCTC^{tri} and lCTCs^{multi} [24,25]. These two subtypes of CTCs harbored completely different mutation patterns and SMPs. sCTCs^{tri} showed significantly higher frequency of mutated KRAS gene and more abundant mutations in Rap1 pathway, whereas significant mutations of MET gene and its downstream PI3K/AKT axis were identified in lCTCs^{multi}. Moreover, SMARCB1 mutation was observed exclusively in lCTCs^{multi}, suggesting the abnormal chromatin remodeling in lCTCs^{multi} [26].

The mutated GTPase-KRAS gene and another GTPase-mediated Rap1 pathway, which are the main features of sCTCs^{tri}, were demonstrated to drive development of therapeutic resistance in various types of neoplasm [22,27,28]. In GC, KRAS gene frequently mutates in chemotherapy-resistant mucinous adenocarcinomas [29]. Similarly, in HER2-positive metastatic GC, the higher frequently mutated KRAS gene was also found in the targeted therapy-resistant patients, more than in sensitive subjects [30]. Mechanism studies showed that the activated KRAS gene can promote EMT which facilitates transition of GC cells to CSCs, which accordingly leads to therapeutic resistance [10]. Moreover, the RAS gene may also induce therapeutic resistance by cooperating with another GTPase-RAP1 to initiate and sustain the ERK signaling pathway [11]. Indeed, activation of the Rap1 pathway was frequently observed in etoposide and cisplatin resistant GC [31].

Abnormal functions of the growth factor receptor MET gene and its downstream PI3K/AKT axis [32], which was mainly found in lCTCs^{multi}, constitute another canonical therapeutic resistance mechanism in GC

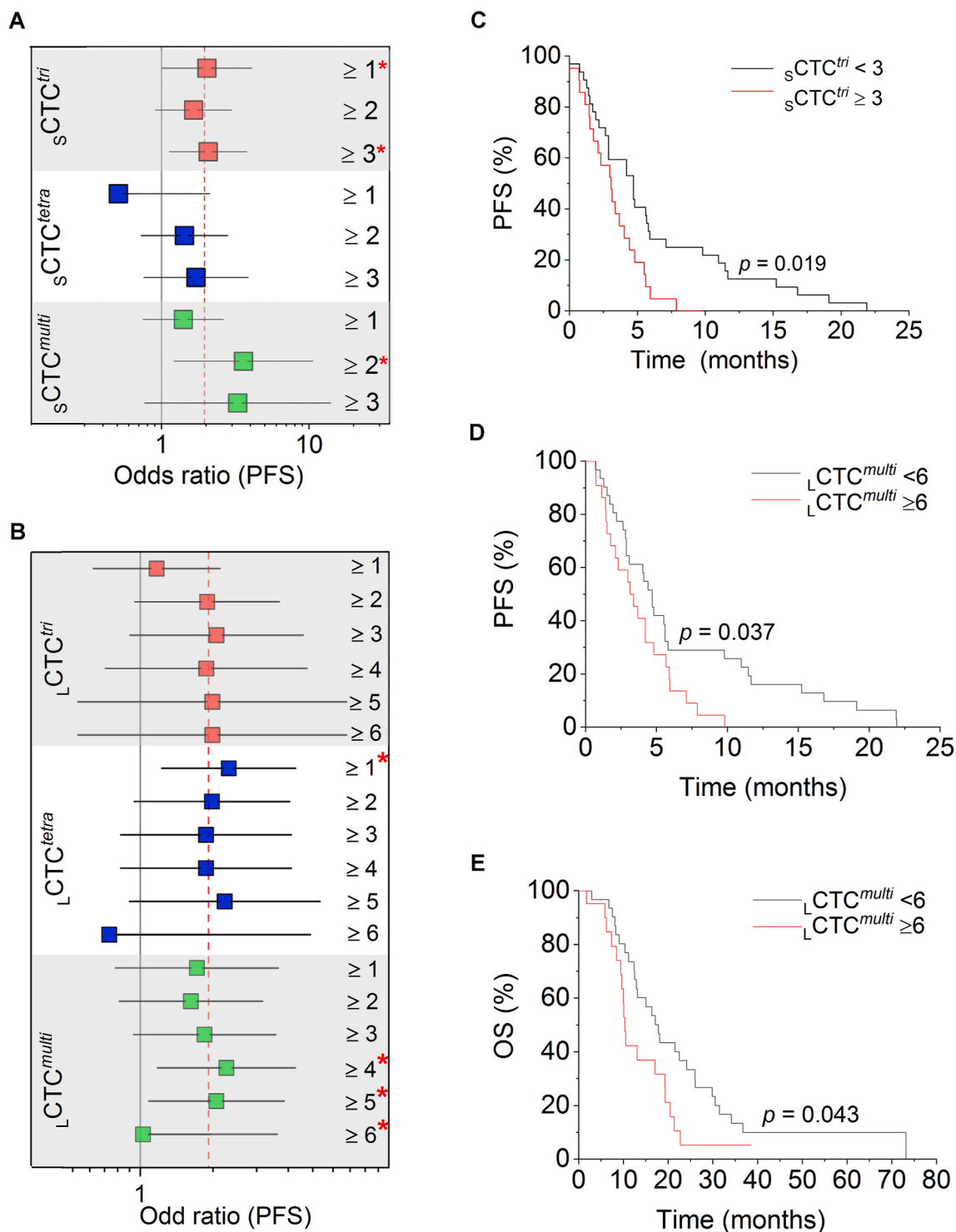


Fig. 2. Increased $sCTCs^{tri}$ and $lCTCs^{multi}$ quantity significantly correlate with poor prognosis in GC. (A–B) Forest plots indicate the association of aneuploid $sCTC$ (A) or $lCTC$ (B) with progression-free survival (PFS) at different CTC cut-off values. Cut-off values varying from 1 to 3 cells for $sCTCs^{tri}$ (A) and 1 to 6 cells for $lCTCs^{multi}$ (B) are respectively examined. Odds ratio is odds of unfavorable cohort ($sCTCs^{tri} \geq$ cut-off value of 1–3 (A) or $lCTCs^{multi} \geq$ cut-off value of 1–6 (B)) versus the odds in the favorable cohort ($sCTCs^{tri} < 1$ to 3 or $lCTCs^{multi} < 1$ to 6). (C–D) Kaplan-Meier curves of PFS in relation to $sCTCs^{tri}$ (C) or $lCTCs^{multi}$ (D) enumeration. (E) Kaplan-Meier curves of OS in relation to $lCTCs^{multi}$ quantity. The cutoff values adopted in (C), (D) and (E) are 3 cells/6 mL for $sCTCs^{tri}$ and 6 cells/6 mL for $lCTCs^{multi}$. Patients with $\geq 3 sCTCs^{tri}$ have significantly shorter PFS than those with $sCTCs^{tri} < 3$, while patients with $\geq 6 lCTCs^{multi}$ shows both shorter PFS and OS compared with those with $< 6 lCTCs^{multi}$.

[32]. Aberrant mutation or amplification of the *MET* gene continuously activates PI3K/AKT axis and thereby enables GC tumor cells to acquire resistance to chemo-/targeted therapy, hence inducing cell death and reducing therapeutic effectiveness [33]. Accordingly, the inhibition of

the MET/PI3K/AKT axis has been recognized as a potential strategy to reverse GC resistance [34].

Aside from the MET/PI3K/AKT axis, the mutated *SMARCB1* gene was found exclusively in $lCTCs^{multi}$. The *SMARCB1* gene, known as the

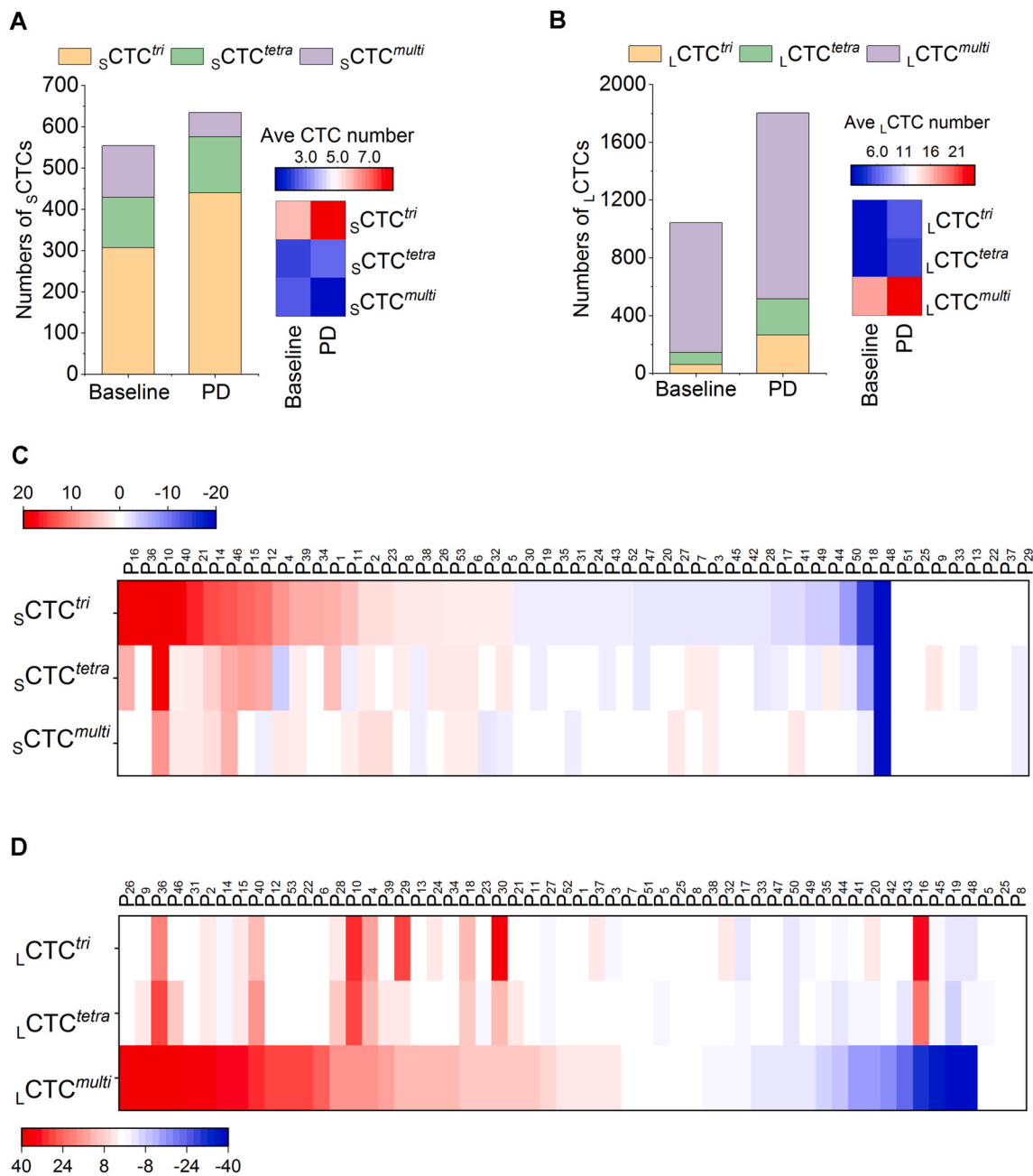


Fig. 3. Chr8 triploid $sCTCs^{tri}$ and multiploid $lCTCs^{multi}$ are the principal subtypes of CTCs involved in therapeutic resistance in GC. (A–B) Quantitative comparison of different chr8 aneuploidy in $sCTCs$ (A) or $lCTCs$ (B) prior to treatment (baseline) and post progressive disease (PD). The histograms and heatmaps respectively indicate total and average number of the aneuploidies at baseline and post PD. (C and D) A heatmap shows quantitative variations in aneuploid $sCTCs$ (C) or $lCTCs$ (D) prior to treatment and post PD in individual PD patient. Increased or decreased CTC numbers are respectively indicated by red or blue color in the heatmap; the white color represents no detectable CTC.

integrase interactor 1 (INI1), is an important subunit of the SWI/SNF (Switch/sucrose non-fermentable) chromatin remodeling complexes [35] SWI/SNF plays an important role in transcriptionally controlling drug resistance [36]. Loss of *SMARCB1* in SWI/SNF complexes may induce up-regulation of multidrug resistance pump *ABCB1* gene, resulting in doxorubicin resistance in human haploid cells [23]. Because loss of *SMARCB1* leads to EZH2 (Enhancer of zeste 2 polycomb repressive complex 2 subunit)-mediated proliferation in tumor cells [37], EZH inhibitor, tazemetostat, has shown encouraging anti-tumor activity in *SMARCB1*-deficient solid tumors [38], which might provide a potential strategy for the treatment of GC as well.

Apparently, dysregulation of multiple pathways, rather than a single pathway, is always involved in therapeutic resistance. However, how

these mechanisms function to foster constant resistance of tumor cells to therapeutic pressures is still unknown. The current study demonstrated that CTCs in different cell sizes possess distinct mechanisms to participate in therapeutic resistance. Dysregulation of the *KRAS* gene and the related-GTPase pathways constitutes the predominant mechanism that contribute to the therapeutic resistance in $sCTCs^{tri}$, whereas abnormal functions of MET/PI3K/AKT axis and *SMARCB1*-mediated chromatin remodeling mainly participate in the therapeutic resistant in $lCTCs^{multi}$ (Fig. 5). Additional studies are required to further investigate the dynamic evolution of these mechanisms throughout treatments by using both baseline and therapeutic resistant clinical specimens. Moreover, single-cell RNA sequencing should be performed to pinpoint specific upregulated genes in $sCTCs^{tri}$ and $lCTCs^{multi}$, which may provide

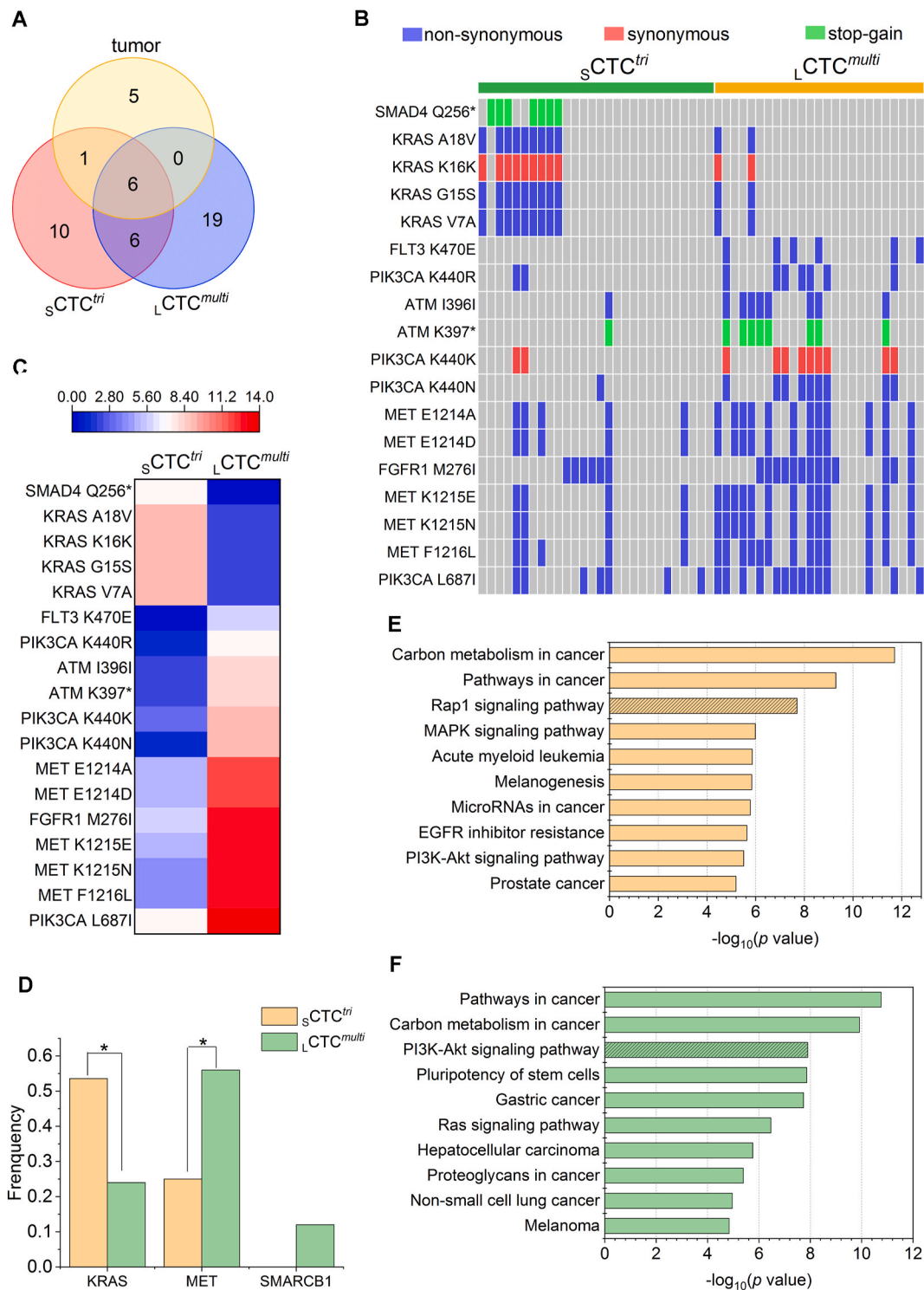


Fig. 4. $sCTCs^{tri}$ and $lCTCs^{multi}$ display distinct mutational signatures and significant mutated pathways (SMPs) identified by single cell targeted sequencing. (A) Venn diagram illustrates the number of gene variations in matched primary tumors, $sCTCs^{tri}$ and $lCTCs^{multi}$ from 2 patients. The overlapping area indicates the number of gene variations shared among samples. (B) Comparison of frequency of mutations in individual $sCTCs^{tri}$ and $lCTCs^{multi}$. (C) Heatmap compares the proportions of $sCTCs^{tri}$ and $lCTCs^{multi}$ carrying mutations in all the sequenced $sCTCs^{tri}$ or $lCTCs^{multi}$ shown in (B) (D) Comparison of mutated genes in $sCTCs^{tri}$ and $lCTCs^{multi}$. In (B), (C) and (D), only the mutational signatures (B–C) or mutated genes (D) that are significantly different between $sCTCs^{tri}$ and $lCTCs^{multi}$ are listed. (E–F) Top 10 SMPs in $sCTCs^{tri}$ and $lCTCs^{multi}$ are analyzed by the KEGG pathways mapper. The p values were calculated using Fisher’s exact test and depicted on a log scale ($-\log_{10} P$ value). The P values of all the listed pathways are lower than 0.05 ($P < 0.05$).

potential novel therapeutic targets in GC.

In conclusion, our study demonstrated that heterogeneous-sized GC CTCs bear distinct karyotypic features, which contribute to chemo-/therapeutic resistance via diverse mechanisms. In $sCTCs^{tri}$, the

dysregulated KRAS gene and the relative GTPase-mediated signaling pathway mainly contribute to the chemo-/targeted therapeutic resistance and poor prognosis in GC patients. However, MET/PI3K/AKT axis activation and abnormal SMARCB1-mediated chromatin remodeling

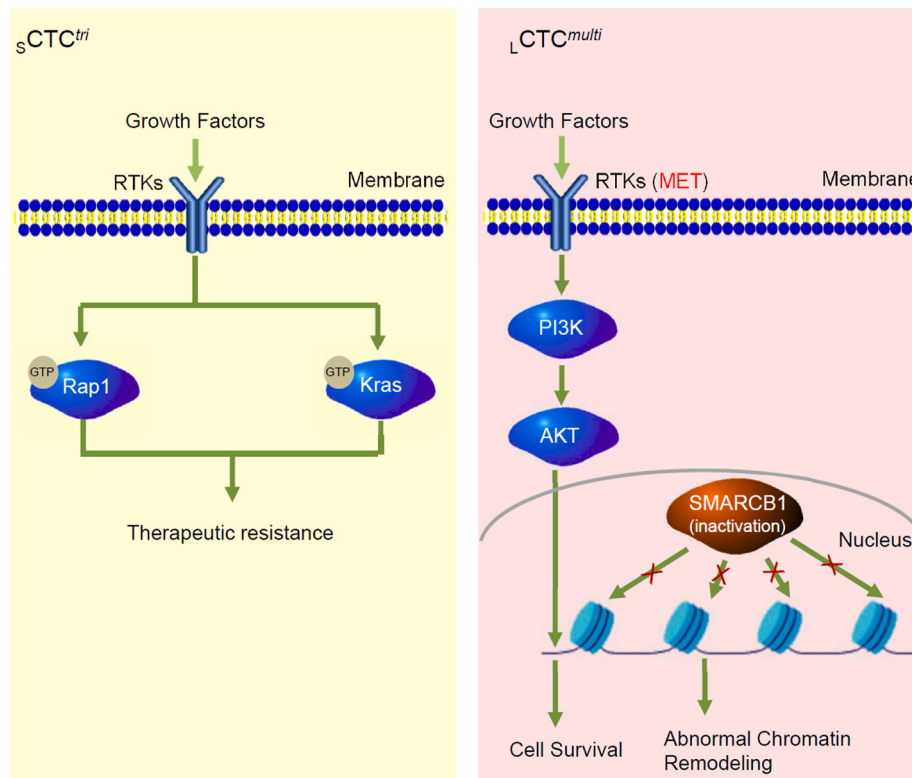


Fig. 5. The diagram depicts different therapeutic resistant mechanisms in $sCTCs^{tri}$ and $lCTCs^{multi}$, respectively. In $sCTCs^{tri}$ (left panel), the dysregulated *KRAS* gene and the relative GTPase-mediated RAP1 signaling pathway mainly contribute to the chemo-/targeted therapeutic resistance and inferior prognosis. In $lCTCs^{multi}$ (right panel), activation of MET/PI3K/AKT axis and abnormal *SMARCB1*-mediated chromatin remodeling promote development of therapeutic resistance in GC.

constitute the principal therapy-resistance mechanism in $lCTCs^{multi}$. Longitudinal profiling of CTCs in terms of morphologic and genomic heterogeneity will facilitate the identification of dominant CTC subtypes relevant to therapy resistance, thereby improving treatment strategies and efficacy.

Authors' contributions

Conception and design: YL, LS; Development of methodology: YL, DW, ST, SL, PL; Acquisition of data (provided animals, acquired and managed patients, provided facilities, etc.): YC, CQ, CZ, DL; Analysis and interpretation of data (e.g., statistical analysis, biostatistics, computational analysis): YC, YD, YF, VK; Writing, review, and/or revision of the manuscript: YC, YL, ZP, JG, XZ, JL; Study supervision: YL, LS.

Declaration of competing interest

iFISH is the registered trademark of Cytelligen. Dr. Peter P. Lin is president at Cytelligen. None of the other authors owns Cytelligen's or Cowin's stock shares. This study was not funded by any of these commercial entities. The other authors declare that they have no potential conflicts of interest.

Acknowledgments

This work was supported by the National Key R&D Program of China (2017YFC1309000, 2017YFC1308900), the Major Program of National Natural Science Foundation of China (91959205), the Project of State Key Laboratory of Radiation Medicine and Protection, Soochow University (No. GZK1201801), the National Natural Science Foundation of China (No. 81301323, No. 81802327 and No. 81872341), the Post-doctoral Research Foundation of China (CN) (2019M660009), Wu Jieping Medical Foundation (320.6750.2021-02-15) and the Capital's

Funds for Health Improvement and Research (2020-1-1022). The funder had no role in study design, data collection and analysis, decision to publish, or preparation of the manuscript. The authors thank staffs at Cytelligen (San Diego, CA) and Cytointelligen (China Medical City, Taizhou, Jiangsu, China) for providing technical assistance.

Appendix A. Supplementary data

Supplementary data to this article can be found online at <https://doi.org/10.1016/j.canlet.2021.06.002>.

Abbreviations

CTC	circulating tumor cells
$sCTCs^{tri}$	small chromosome 8 triploid CTCs
$lCTCs^{multi}$	large chromosome 8 multiploid CTCs
CT	computed tomography
EMT	epithelial-to-mesenchymal transition
GC	gastric cancer
HER2	human epidermal growth factor receptor 2
iFISH	immunofluorescence staining-fluorescence in situ hybridization
<i>KRAS</i>	kirsten rat sarcoma 2 viral oncogene homolog
KPS	karnofsky performance status
OS	overall survival
PFS	progression-free survival
PR	partial responses
PD	progressive disease
<i>PIK3C</i>	phosphatidylinositol -4, 5-bisphosphate 3-kinase catalytic subunit alpha
SCS	single cell sequencing
SD	stable disease
SMPs	significantly mutated pathways

References

- [1] L. Keller, K. Pantel, Unravelling tumour heterogeneity by single-cell profiling of circulating tumour cells, *Nat. Rev. Canc.* 19 (2019) 553–567.
- [2] M.G. Krebs, R.L. Metcalf, L. Carter, G. Brady, F.H. Blackhall, C. Dive, Molecular analysis of circulating tumour cells-biology and biomarkers, *Nat. Rev. Clin. Oncol.* 11 (2014) 129–144.
- [3] M. Yu, A. Bardia, B.S. Wittner, S.L. Stott, M.E. Smas, D.T. Ting, S.J. Isakoff, J. C. Ciciliano, M.N. Wells, A.M. Shah, K.F. Concannon, M.C. Donaldson, L.V. Sequist, E. Brachtel, D. Sgroi, J. Baselga, S. Ramaswamy, M. Toner, D.A. Haber, S. Maheswaran, Circulating breast tumor cells exhibit dynamic changes in epithelial and mesenchymal composition, *Science* 339 (2013) 580–584.
- [4] X. Liu, J. Li, B.L. Cadilha, A. Markota, C. Voigt, Z. Huang, P.P. Lin, D.D. Wang, J. Dai, G. Kranz, A. Krandick, D. Libl, H. Zitzelsberger, I. Zagorski, H. Braselmann, M. Pan, S. Zhu, Y. Huang, S. Niedermeier, C.A. Reichel, B. Uhl, D. Briukhovetska, J. Suarez, S. Kobold, O. Gires, H. Wang, Epithelial-type systemic breast carcinoma cells with a restricted mesenchymal transition are a major source of metastasis, *Sci. Adv.* 5 (2019), eaav4275.
- [5] H.E. Danielsen, M. Pradhan, M. Novelli, Revisiting tumour aneuploidy - the place of ploidy assessment in the molecular era, *Nat. Rev. Clin. Oncol.* 13 (2016) 291–304.
- [6] G.J. Kops, B.A. Weaver, D.W. Cleveland, On the road to cancer: aneuploidy and the mitotic checkpoint, *Nat. Rev. Canc.* 5 (2005) 773–785.
- [7] N. McGranahan, R.A. Burrell, D. Endesfelder, M.R. Novelli, C. Swanton, Cancer chromosomal instability: therapeutic and diagnostic challenges, *EMBO Rep.* 13 (2012) 528–538.
- [8] Y. Li, X. Zhang, S. Ge, J. Gao, J. Gong, M. Lu, Q. Zhang, Y. Cao, D.D. Wang, P.P. Lin, L. Shen, Clinical significance of phenotyping and karyotyping of circulating tumor cells in patients with advanced gastric cancer, *Oncotarget* 5 (2014) 6594–6602.
- [9] Y. Li, X. Zhang, D. Liu, J. Gong, D.D. Wang, S. Li, Z. Peng, Y. Li, X. Wang, P.P. Lin, M. Li, L. Shen, Evolutionary expression of HER2 conferred by chromosome aneuploidy on circulating gastric cancer cells contributes to developing targeted and chemotherapeutic resistance, *Clin. Canc. Res.* 24 (2018) 5261–5271.
- [10] C. Yoon, J. Till, S.J. Cho, K.K. Chang, J.X. Lin, C.M. Huang, S. Ryeom, S.S. Yoon, KRAS activation in gastric adenocarcinoma stimulates epithelial-to-mesenchymal transition to cancer stem-like cells and promotes metastasis, *Mol. Canc. Res.* 17 (2019) 1945–1957.
- [11] A. Diaz-Serrano, B. Angulo, C. Dominguez, R. Pazo-Cid, A. Salud, P. Jimenez-Fonseca, A. Leon, M.C. Galan, M. Alsina, F. Rivera, J.C. Plaza, L. Paz-Ares, F. Lopez-Rios, C. Gomez-Martin, Genomic profiling of HER2-positive gastric cancer: PI3K/Akt/mTOR pathway as predictor of outcomes in HER2-positive advanced gastric cancer treated with trastuzumab, *Oncol.* 23 (2018) 1092–1102.
- [12] G. Attard, J.S. de Bono, Utilizing circulating tumor cells: challenges and pitfalls, *Curr. Opin. Genet. Dev.* 21 (2011) 50–58.
- [13] D. Marrinucci, K. Bethel, D. Lazar, J. Fisher, E. Huynh, P. Clark, R. Bruce, J. Nieva, P. Kuhn, Cytomorphology of circulating colorectal tumor cells: a small case series, *J. Oncol.* 2010 (2010) 861341.
- [14] J.P. Thiery, C.T. Lim, Tumor dissemination: an EMT affair, *Canc. Cell* 23 (2013) 272–273.
- [15] L. Zhang, X. Zhang, Y. Liu, T. Zhang, Z. Wang, M. Gu, Y. Li, D.D. Wang, W. Li, P. P. Lin, PD-L1(+) aneuploid circulating tumor endothelial cells (CTECs) exhibit resistance to the checkpoint blockade immunotherapy in advanced NSCLC patients, *Canc. Lett.* 469 (2020) 355–366.
- [16] J.F. Chen, H. Ho, J. Lichterman, Y.T. Lu, Y. Zhang, M.A. Garcia, S.F. Chen, A. J. Liang, E. Hodara, H.E. Zhou, S. Hou, R.S. Ahmed, D.J. Luthringer, J. Huang, K. C. Li, L.W. Chung, Z. Ke, H.R. Tseng, E.M. Posadas, Subclassification of prostate cancer circulating tumor cells by nuclear size reveals very small nuclear circulating tumor cells in patients with visceral metastases, *Cancer* 121 (2015) 3240–3251.
- [17] L. Wang, Y. Li, J. Xu, A. Zhang, X. Wang, R. Tang, X. Zhang, H. Yin, M. Liu, D. D. Wang, P.P. Lin, L. Shen, J. Dong, Quantified postsurgical small cell size CTCs and EpCAM(+) circulating tumor stem cells with cytogenetic abnormalities in hepatocellular carcinoma patients determine cancer relapse, *Canc. Lett.* 412 (2018) 99–107.
- [18] Y. Li, J. Gong, Q. Zhang, Z. Lu, J. Gao, Y. Li, Y. Cao, L. Shen, Dynamic monitoring of circulating tumour cells to evaluate therapeutic efficacy in advanced gastric cancer, *Br. J. Canc.* 114 (2016) 138–145.
- [19] Y. Li, X. Zhang, J. Gong, Q. Zhang, J. Gao, Y. Cao, D.D. Wang, P.P. Lin, L. Shen, Aneuploidy of chromosome 8 in circulating tumor cells correlates with prognosis in patients with advanced gastric cancer, *Chin. J. Canc. Res.* 28 (2016) 579–588.
- [20] J. Reimand, R. Isserlin, V. Voisin, M. Kucera, C. Tannus-Lopes, A. Rostamianfar, L. Wadi, M. Meyer, J. Wong, C. Xu, D. Merico, G.D. Bader, Pathway enrichment analysis and visualization of omics data using g:Profiler, GSEA, Cytoscape and EnrichmentMap, *Nat. Protoc.* 14 (2019) 482–517.
- [21] U. Raudvere, L. Kolberg, I. Kuzmin, T. Arak, P. Adler, H. Peterson, J. Vilo, g:Profiler: a web server for functional enrichment analysis and conversions of gene lists (2019 update), *Nucleic Acids Res.* 47 (2019) W191–W198.
- [22] S. Shah, E.J. Brock, K. Ji, R.R. Mattingly, Ras and Rap1: a tale of two GTPases, *Semin. Canc. Biol.* 54 (2019) 29–39.
- [23] R. Dubey, A.M. Lebensohn, Z. Bahrami-Nejad, C. Marceau, M. Champion, O. Gevaert, B.I. Sikic, J.E. Carette, R. Rohatgi, Chromatin-remodeling complex SWI/SNF controls multidrug resistance by transcriptionally regulating the drug efflux pump ABCB1, *Canc. Res.* 76 (2016) 5810–5821.
- [24] D.T. Miyamoto, Y. Zheng, B.S. Wittner, R.J. Lee, H. Zhu, K.T. Broderick, R. Desai, D.B. Fox, B.W. Brannigan, J. Trautwein, K.S. Arora, N. Desai, D.M. Dahl, L. V. Sequist, M.R. Smith, R. Kapur, C.L. Wu, T. Shioda, S. Ramaswamy, D.T. Ting, M. Toner, S. Maheswaran, D.A. Haber, RNA-Seq of single prostate CTCs implicates noncanonical Wnt signaling in antiandrogen resistance, *Science* 349 (2015) 1351–1356.
- [25] D. Boral, M. Vishnoi, H.N. Liu, W. Yin, M.L. Sprouse, A. Scamardo, D.S. Hong, T. Z. Tan, J.P. Thiery, J.C. Chang, D. Marchetti, Molecular characterization of breast cancer CTCs associated with brain metastasis, *Nat. Commun.* 8 (2017) 196.
- [26] M. Pancione, A. Remo, C. Zanella, L. Sabatino, A. Di Blasi, C. Laudanna, L. Astati, M. Rocco, D. Bifano, P. Piacentini, L. Pavan, A. Purgato, F. Greco, A. Talamini, A. Bonetti, M. Ceccarelli, R. Vendraminelli, E. Manfrin, V. Colantuoni, The chromatin remodelling component SMARCB1/INI1 influences the metastatic behavior of colorectal cancer through a gene signature mapping to chromosome 22, *J. Transl. Med.* 11 (2013) 297.
- [27] K.M. Haigis, KRAS alleles: the devil is in the detail, *Trends Canc.* 3 (2017) 686–697.
- [28] C.A. Stalneck, C.J. Der, RAS, wanted dead or alive: advances in targeting RAS mutant cancers, *Sci. Signal.* 13 (2020).
- [29] L.C. Hewitt, Y. Saito, T. Wang, Y. Matsuda, J. Oosting, A.N.S. Silva, H.L. Slaney, V. Melotte, G. Hutchins, P. Tan, T. Yoshikawa, T. Arai, H.I. Grabsch, KRAS status is related to histological phenotype in gastric cancer: results from a large multicentre study, *Gastric Cancer* 22 (2019) 1193–1203.
- [30] F. Pietrantonio, G. Fuca, F. Morano, A. Ghoghini, S. Corso, G. Aprile, F. Perrone, F. De Vita, E. Tamborini, G. Tomasello, A.V. Gualeni, E. Ongaro, A. Busico, E. Gommoni, C.C. Volpi, M.M. Laterza, S. Corallo, M. Prisciandaro, M. Antista, A. Pellegrinelli, L. Castagnoli, S.M. Pupa, G. Pruneri, F. de Braud, S. Giordano, C. Cremolini, M. Di Bartolomeo, Biomarkers of primary resistance to trastuzumab in HER2-positive metastatic gastric cancer patients: the AMNESIA case-control study, *Clin. Canc. Res.* 24 (2018) 1082–1089.
- [31] X. Li, W. Liu, H. Wang, L. Yang, Y. Li, H. Wen, H. Ning, J. Wang, L. Zhang, J. Li, D. Fan, Rap1 is indispensable for TRF2 function in etoposide-induced DNA damage response in gastric cancer cell line, *Oncogenesis* 4 (2015) e144.
- [32] C.A. Bradley, M. Salto-Tellez, P. Laurent-Puig, A. Bardelli, C. Rolf, J. Taberero, H.A. Khawaja, M. Lawler, P.G. Johnston, S. Van Schaejbroeck, M.E. consortium, Targeting c-MET in gastrointestinal tumours: rationale, opportunities and challenges, *Nat. Rev. Clin. Oncol.* 14 (2017) 562–576.
- [33] Y.Y. Lee, H.P. Kim, M.J. Kang, B.K. Cho, S.W. Han, T.Y. Kim, E.C. Yi, Phosphoproteomic analysis identifies activated MET-axis PI3K/AKT and MAPK/ERK in lapatinib-resistant cancer cell line, *Exp. Mol. Med.* 45 (2013) e64.
- [34] D. Chen, X. Lin, C. Zhang, Z. Liu, Z. Chen, Z. Li, J. Wang, B. Li, Y. Hu, B. Dong, L. Shen, J. Ji, J. Gao, X. Zhang, Dual PI3K/mTOR inhibitor BEZ235 as a promising therapeutic strategy against paclitaxel-resistant gastric cancer via targeting PI3K/Akt/mTOR pathway, *Cell Death Dis.* 9 (2018) 123.
- [35] D. Reisman, S. Glaros, E.A. Thompson, The SWI/SNF complex and cancer, *Oncogene* 28 (2009) 1653–1668.
- [36] R.H. Wijdeven, B. Pang, S.Y. van der Zanden, X. Qiao, V. Blomen, M. Hoogstraat, E. H. Lips, L. Janssen, L. Wessels, T.R. Brummelkamp, J. Neefjes, Genome-wide identification and characterization of novel factors conferring resistance to topoisomerase II poisons in cancer, *Canc. Res.* 75 (2015) 4176–4187.
- [37] M. Gounder, P. Schöffski, R.L. Jones, M. Agulnik, G.M. Cote, V.M. Villalobos, S. Attia, R. Chugh, T.W.-W. Chen, T. Jahan, E.T. Loggers, A. Gupta, A. Italiano, G. D. Demetri, R. Ratan, L.E. Davis, O. Mir, P. Dileo, B.A. Van Tine, J.G. Pressey, T. Lingaraj, A. Rajarethinam, L. Sierra, S. Agarwal, S. Stacchiotti, Tazemetostat in advanced epithelioid sarcoma with loss of INI1/SMARCB1: an international, open-label, phase 2 basket study, *Lancet Oncol.* 21 (2020) 1423–1432.
- [38] F. Morschhauser, H. Tilly, A. Chaidos, P. McKay, T. Phillips, S. Assouline, C. L. Batlevi, P. Campbell, V. Ribrag, G.L. Damaj, M. Dickinson, W. Jurczak, M. Kazmierczak, S. Opat, J. Radford, A. Schmitt, J. Yang, J. Whalen, S. Agarwal, D. Adib, G. Salles, Tazemetostat for patients with relapsed or refractory follicular lymphoma: an open-label, single-arm, multicentre, phase 2 trial, *Lancet Oncol.* 21 (2020) 1433–1442.